ACS APPLIED MATERIALS & INTERFACES

Research Article

www.acsami.org

Evenly Distributed Thin-Film Ag Coating on Stainless Plate by Tricomponent Ag/Silicate/PU with Antimicrobial and Biocompatible Properties

Yi-Hsiu Huang,[‡,⊥] Mark Hung-Chih Chen,[†,⊥] Bing-Heng Lee,[†] Kuo-Huang Hsieh,[§] Yuan-Kun Tu,[∥] Jiang-Jen Lin,[‡] and Chih-Hao Chang*[,†]

[†]Department of Orthopedics, National Taiwan University Hospital and National Taiwan University College of Medicine, Taipei 10002, Taiwan

[‡]Institute of Polymer Science and Engineering, National Taiwan University, Taipei 10617, Taiwan

[§]Department of Chemical Engineering, National Taiwan University, Taipei 10617, Taiwan

[∥]Department of Orthopedics, Department of Biomedical Engineering, E-DA Hospital, I-Shou University, Kaohsiung 82445, Taiwan

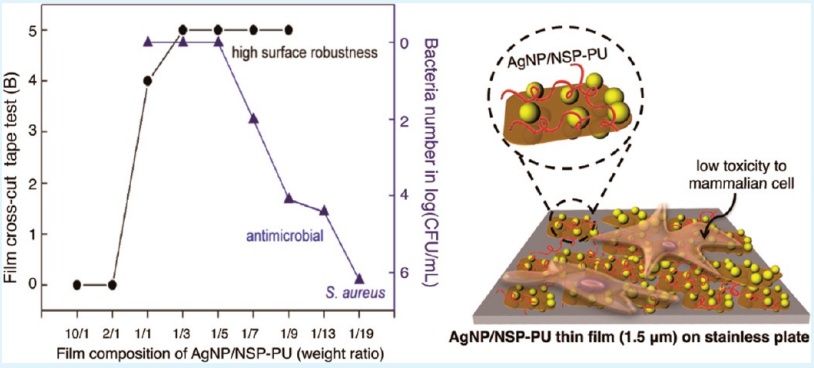

ABSTRACT: A tricomponent nanohybrid dispersion in water comprising silver nanoparticles (AgNP), nanometer-thick silicate platelets (NSP), and water-based polyurethane (PU) was developed for surface coating on orthopedic metal plates. The previously developed AgNP-on-NSP nanohybrid was homogeneously blended into a selected waterborne PU dispersion at varied weight ratios from 1/0.1 to 1/10 (w/w). PU was used to adhere the Ag nanohybrid to the metal surface. The resultant dispersions were analyzed and found to contain AgNP 2−18 nm in diameter and characterized by using UV absorption and TEM micrograph. The subsequent coating of AgNP/NSP−PU dispersion generated a film of 1.5 μm thickness on the metal plate surface, further characterized by an energy dispersive spectroscope (EDS) to show the homogeneous distribution of Ag, Si, and C elements on the metal plates. The surface antimicrobial efficacy was proven for the coating composition of AgNP/NSP to PU ranging from 1/1 to 1/5 by weight ratio but irrelevant to the thickness of the coated materials. The metal plate coated with the high Ag content at 1/1 (w/w) ratio was shown to have very low cytotoxicity toward the contacted mammal fibroblasts. Overall, the optimized tricomponent Ag/silicate/PU in water dispersion from 1/2 to 1/3 (w/w) could generate a stable film on a metal surface exhibiting both antimicrobial and biocompatible properties. The facile coating technique of the AgNP/NSP in waterborne PU is proven to be viable for fabricating infection- and cytotoxicity-free medical devices.

KEYWORDS: *nanosilicate platelets (NSP), silver nanoparticles (AgNP), waterborne polyurethane (PU), antibacterial, medical device, stainless plate, surface treatment*

1. INTRODUCTION

Stainless steel has been widely used as the standard material in bone fracture patients due to its excellent mechanical properties and corrosion resistance. However, one of the major drawbacks of using such a metal material as an orthopedic plate is its surface accessibility for possible bacterial infections. Osteomyelitis could occur through two mechanistic steps: Initially, the bacteria invade the body and transmit through the blood to the plate site. Second, the bacteria adhere onto the plate and proliferate locally. In conventional treatments, antibiotics are commonly used to overcome the problem of bacterial invasion. It is highly desired to resolve this problem by surface treatment of the metal to fabricate infection-free medical devices. The presence of coated antimicrobial agents may gain the advantages of reducing the risk of infections from open wounds and surgical conditions during and after the surgery.

Silver compounds as antimicrobial agents are widely used for surface treatments of various materials. Metallic materials of

Received: August 29, 2014
Accepted: October 10, 2014
Published: October 10, 2014

biomedical devices in the fields of surgery include stainless steel, titanium, and titanium alloys. These materials are generally susceptible to bacterial adhesion resulting in infection of the tissues. Such biomedical-related infections often require removal and replacement of the devices and immediate antibiotic therapy to avoid the development of severe complications such as osteomyelitis.[1] In order to fabricate infection-resistant medical devices, the metal surface can be treated with antimicrobial agents using different surface treatment techniques.[2−6] In the recent advances in nanotechnology, different metallic nanoparticles were found to be effective for antimicrobial functions.[3] The metallic nanoparticles were prepared by various methods such as electron beam and photoinductions,[7] as well as chemical reductions with reducing agents.[8] The antimicrobial efficacy is often attributed to the nature of the nanoparticles, including particle size, uniformity of size distributions, stabilizers, and the tendency of particle aggregation.[9−11] Homogeneous dispersion of the nanoparticles in polymer matrices was important for the downstream uses.[12,13] In addition, the avoidance of using organic solvents in the synthetic process was preferred owing to the concerns for their potential carcinogenic and environmental impacts.[14,15]

Previously, we prepared the silver nanoparticles (AgNP) in the presence of the nanometer-thick silicate platelets, which were derived from the multilayered clays through the exfoliation process involving water-soluble polymers.[16] The nanoplatelets formed of silicate clays could serve as high-surface-area supports during the formation of AgNP under the reducing process. The AgNP supported on silicates were organic-free after purification. Without the organic matter, the naked AgNP was directly associated with the silicate nanoplatelets and homogeneously dispersible in water.[17]

On the other hand, the literature had revealed the coating of silver-based nanoparticles on stainless steel by using plasma and positively charged micelles by plasma spray on titanium alloy substrates.[18−20] But few reports had addressed the side effect of Ag^+ leaching, stability, or AgNP cytotoxicity.[21] It is not clear yet whether the possible biological toxicity may be related to nanoparticles directly or to the released Ag^+ ion species. Further, it was also reported that the toxicity of AgNP may cause damage to cell membranes and oxidative stress to cells, or these may occur through the interactions of Ag^+ ions with thio-protein.[8,22] The Ag size was considered to be the predominant factor affecting bactericidal activity and cell toxicity. In general, the smaller particle size and homogeneous dispersion contributed to the enhancement of antibacterial efficacy.[23,24] However, it was also documented that AgNP could exhibit cytotoxic and genotoxic effects in mammalian cells.[25,26] Their accumulation in the mitochondria and nuclei of fibroblasts or glioblastoma cells may lead to excessive production of reactive oxygen species and cellular damage.[27] Small AgNPs (>20 nm) were found to up-regulate the expressions of proinflammatory genes and induce the immune response of macrophages.[25] The Ag toxicity due to the exposure of inhalation, instillation, skin contact, or oral intake was reviewed for various tests in vivo and in vitro.[28,29] The toxicity was related to the shape, size, and composition of AgNPs that pose different risks to human health and environmental impact. It was reported that the possible mechanism of AgNP cytotoxicity is due to reactive oxygen species (ROS) generation.[8] Hence, the control of Ag size and reducing form in a stabilized manner during the applications of implant coating is an important issue.

In our earlier studies, we investigated the method of stabilizing AgNPs in water by utilizing the silicate clays as the supports for AgNPs.[30,31] The nanohybrids of AgNPs on the inorganic support of nanoscale silicate platelet from the natural clay (AgNP/NSP) have been formulated in waterborne PU polymer as the coating material. The coated surface of stainless steel implants was characterized for physical properties and antimicrobial efficacy. The role of NSP to mitigate the side effect of AgNP toxicity was demonstrated. The waterborne PU served the function of Ag adhesion onto the metal plate surface. The developments of the ternary AgNP/NSP−PU nanomaterial and the facile coating process will benefit the future use of biomedical devices.

2. EXPERIMENTAL SECTION

2.1. Synthesis of AgNP/NSP Nanohybrids. Sodium montmorillonite (MMT), a natural smectite aluminosilicate, was obtained from Nanocor, Inc. This bentonite clay has a generic structure of 2:1 layered silicate oxide and aluminum oxides at two tetrahedral sheets sandwiching an edge-shared octahedral sheet in geometric arrangement. The capacity of exchangeable cationic species (i.e., CEC) or exchangeable Na^+ capacity was estimated to be 1.20 mequiv/g. The clay's layered structure could be exfoliated or randomized by using a polymeric form of poly(oxypropylene)-polyamine HCl salt to yield nanoscale silicate platelets (NSP) in water dispersion. The exfoliation or delamination of Na^+-MMT clay minerals into NSP in water dispersion was followed by purification procedures involving a biphasic extraction step to remove the organic polyamines.[32] After the purification, the exfoliated silicate platelets were characterized as very thin platelets of geometric shape with the lateral dimension of 100 × 100 × 1 nm, and the content of ionic charges was 18 000 ions per platelet. By using NSP as the physical support, AgNP was prepared at the composition weight ratio of AgNP/NSP 7/93 (w/w). The typical procedures are described in the following. To a three-necked, round-bottom flask equipped with mechanical stirring, a reflux condenser, a heating mantle, and a nitrogen inlet−outlet line was added the slurry of NSP (187 g, 9.9 wt % in deionized water). Under vigorous agitation at 300−600 rpm of mechanical stirring, $AgNO_3$ solution (14.7 g, 15.0 wt % in water) was added in a dropwise manner. The mixtures were slowly heated to 80 °C, and this temperature was maintained for 4 h. The formation of Ag^0 particles were monitored by UV−visible absorption on Hitachi U-4100 spectrophotometer. When the absorption reached its maximum at the 408 nm peak, the reaction was terminated by cooling the solution to ambient temperature. The particle sizes were measured by a transmission electron microscope (TEM, JEOL JEM-1230) operating at 100 kV and with a Gatan DualVision CCD camera. The size distribution was estimated from 100 individual particles.

2.2. Synthesis of Biodurable Waterborne PU. The synthetic procedures for selecting waterborne PU were briefly described as follows. Generally, the PU prepolymers were prepared by the reaction of isophorone diisocyanate (IPDI) and polyester-polyols or poly(propylene) glycol at a molecular weight of 2000 (i.e., PPG2000) at stoichiometric equivalents. The designated IPDI amount was first added into a reaction kettle and heated to melt for homogeneity. The corresponded amount of polyol was followed and mixed with IPDI under agitation. The reaction generally occurred under dry nitrogen atmosphere at approximately 60 °C. The isocyanate content in IPDI reaction mixture was determined by using di-*n*-butyl amine titration method. Using comonomers of dimethylol propionic acid (DMPA) and ethylenediamine (EDA) as chain extender and the subsequent addition of triethylamine (TEA), the adjustable hydrophilic property of the water-dispersible PU was obtained. The molecular weight of PU monomer in this study is about 40 000−60 000. The specific stoichiometric ratio of IPDI/PPG2000/DMPA/EDA/TEA in the monomer equivalent ratio of 4:3:0.4:0.6:0.4 was the optimization in this study.

2.3. Coating of AgNP/NSP−PU on Metal Plates. The waterborne PU was used to blend with an aliquot of AgNP/NSP dispersion at the designated weight ratio. Eight formulations of AgNP/NSP to PU were

prepared from the mixing of AgNP/NSP and PU at different weight ratios of 1:0.1, 1:0.5, 1:1, 1:3, 1:5, 1:7, 1:9, and 1:10. The drop-coating method of applying the nanohybrid dispersion on a stainless steel plate surface was developed. By using the same procedure, various films were generated in different thicknesses by casting the nanohybrid/PU slurry solution on a 3 × 3 or 1 × 1 cm stainless steel (316L) and dried at room temperature for 24 h.

2.4. Surface Characterization of AgNP/NSP−PU Film. Cross-cut test analyses were measured for the metal plates coated with AgNP/NSP to PU slurry composite (1/0.1 to 1/10 weight ratio). Adhesion of the AgNP/NSP−PU coatings to the metal implant was measured according to ASTM D 3359B-02. The adhesion test kit was purchased from ZEHNTNER (Switzerland). The cutting tool was fitted with a blade containing 11 teeth spaced 1.0 mm apart. The cutting tool was used to make the cross-cut pattern at 90° angles through the coating. The coating was brushed lightly with a soft brush after each cut to remove excess debris from the surface. Permacel 99 tape was applied to the cut surface and rubbed with the eraser end of a pencil to ensure good contact with the coating and then removed after 90s. Samples were captured under a lighted magnifying glass (7× magnification) and rated according to the ASTM rating scheme, shown in Table 1 to clarify.

Table 1. Classification of Adhesion by Cross-Cut Tape Test (ASTM D3359)

AgNP/NSP to PU ratio	classification	percent area removed
1/2, 1/3, 1/4, 1/5, 1/10	5B	0%
1/1	4B	<5%
	3B	5−15%
	2B	15−35%
	1B	35−65%
2/1, 10/1	0B	>65%

Both the coating layer thickness and the silver nanoparticle size were examined by Microfigure Measuring Instrument (Surfcorder ET3000, Kosaka Laboratory Ltd.) and Transmission Electron Microscopy (TEM), respectively. The size of the silver nanoparticles was characterized by TEM. The TEM examination for Ag particle size was performed according to the following procedures. The AgNP/NSP−PU slurry composites were casted from 4 wt % solution on copper grids, dried at 60 °C for 72 h, and vacuumed at 60 °C for 48 h. The specimens were then stained with 2 wt % phosphotungstic acid (Alfa Aesar) for 1 min. The micrographs were obtained by using TEM (JEOL JEM-1230, Japan).

For energy dispersive X-ray spectroscopy (EDS) examination, the samples were prepared from the mixing of AgNP/NSP and PU at different ratios of 1/1, 1/9 (w/w), and using AgNP/NSP as control, then examined the Ag (AgNP), Si (NSP), and C (PU) element distribution property by energy dispersive X-ray spectroscopy (EDS).

To further characterize the surface topography of AgNP/NSP−PU film, we used AFM to monitor the surface morphology. Topography and phase images were recorded simultaneously. The nanoscale morphology of these films is measured with Veeco NanoScope IV MultiMode AFM. The AFM measurements were performed by a multimode instrument connected to Nanoscope IV controller and equipped with E piezoelectric scanner (Veeco Metrology). Contact mode was used to determine the surface roughness of the films. All measurements were performed in tapping mode.

2.5. Antibacterial Analysis and SEM of AgNP/NSP−PU Surface. The antimicrobial efficacy of the AgNP coated surface was investigated by using pathogenic bacterial strains of *Staphylococcus aureus* (American Type Culture Collection (ATCC) 6538), obtained from Department of Clinical Laboratory, Sciences and Medical Biotechnology, College of Medicine, National Taiwan University, Taipei, Taiwan. By employing the standard microdilution method, the bactericidal concentration was defined as the lowest concentration of an antimicrobial agent to prevent the growth of microorganism after subculture onto the antibiotic-free media. The inhibition of bacterial growth was measured according to the National Committee for Clinical Laboratory Standards. Typically, bacteria were incubated overnight and inoculated into 5 mL fresh medium to restart the cell cycle. After 3 h of incubation at 37 °C, the cells were synchronized at the log phase of the growth curve, featured with the optical density at 600 nm (OD_{600}) of 0.3−0.5. After 1000-fold dilution, an aliquot of solution (2 mL) at approximately 1×10^5 colony formation unit per milliliter (CFU mL^{-1}) was spread on Luria−Bertani (LB) agars, in which the tested materials were added at the designed concentrations. Colony numbers were counted after overnight incubation at 37 °C.

The bacterial suspension was diluted about to 1×10^4 CFU mL^{-1} by adding LB for *S. aureus*. Samples (3 × 3 cm) were placed in 6 cm Petri dishes. The inoculum of 2 mL of bacterial suspension was instilled on the surface of the sample. The PU coating and blank stainless steel were two controlled samples. Colony numbers were counted after 0, 3, 6, 12, and 24 h of incubation at 37 °C. Each sample was tested by inoculating the *S. aureus* suspension in a semisolid isotonic LB broth. After 24 h of incubation at 37 °C in a sterile Petri dish, bacterial cells were recovered from the sample surface via elution of the plate. The number of colony forming units (CFUs) was then determined. The effects were recorded as logarithm reduction and compared with the control samples. Each surface of three Ag coated samples (six for the controls) was inoculated with aliquot of *S. aureus*. The resultant CFUs for different samples were recorded in the respective reduction.

The SEM was performed in a Nano230 SEM microscope operated at 10 kV with the metal samples prepared by focused ion beam (FIB) method (Nano 230 SEM). Small pieces of metal plates (3 × 3 cm) with the Ag-coated surface were prepared and mounted on gold (Au) horseshoe grids before being milled to electron transparency in the FIB. The solution of *S. aureus* was diluted to the bacterial number of 1×10^4 CFU mL^{-1}, from which 2 mL of the sample was treated with 2.5% glutaraldehyde and stored overnight at 4 °C. The samples were further dehydrated with 70, 80, 95, and 99.9% ethanol and examined on FE-SEM.

The AgNP/NSP−PU coated metal plates (1 × 1 cm) were soaked in 200 μL of a culture solution of bacteria (approximately 1×10^4 CFU ml^{-1}) for 12 h of contact time under amibient condition. BacLight LIVE/DEAD staining (Invitrogen Ltd., Paisley, U.K.) was used according to the manufacturer's instructions to visualize bacteria viability. Bacteria were observed using a Zeiss A1 upright fluorescence microscope with a 40× objective lens and an Omega XF25 filter (Omega Optical, Brattleboro, VT). Bacterial cells were incubated in the presence of LIVE/DEAD and stained either green (viable) or red (dead).

2.6. Cytotoxicity Test of Tricomponent of AgNP/NSP−PU. An in vitro cytotoxicity test was performed according to modified method of ISO 10993-5. Cell lines of CCL 163 (Balb/3T3 clone A31) were purchased from American Type Culture Collection. The cell toxicity was measured according to the modified method of ISO 10993-5 for medical devices. These test samples were applied to mouse fibroblasts. Cells were seeded in 24-well tissue culture plates at a density of 2×10^4 cells per well. After 24 h, the medium was removed, replaced by 0.1 mL of tested sample (suspension of AgNP/NSP−PU composites) and 0.9 mL of medium, and incubated for another 24 h. The coated AgNP/NSP−PU slurry samples were serial diluted in Dulbecco's modified Eagle's medium (DMEM) supplemented with 10% fetal bovine serum (FBS) and penicillin and streptomycin (100 μg/mL); the final concentrations for treatment were 0.1, 1, 5, and 10 ppm. AgNP/NSP−PU suspension was not used as a control; however, incubating for 24 h at 37 °C without material contact was used as the negative control. All measurements were performed in six repeat wells and were performed independently in triplicate. After incubation at 37 °C in 5% CO_2 for 24 h, a tetrazolium salt splitting test (MTT test) was performed to determine the metabolic activity of the cell culture. The metabolic activity of the cells was determined by colorimetric quantification of the colored tetrazolium salt (MTT) and converted by the mitochondrial dehydrogenases. The optical density of the negative control was standardized at a wavelength of 570 nm at 100% and compared with the relative values of the test sample and the positive control. The absorbance was measured at 570 nm using a microplate reader and normalized to the negative control to obtain cell viability. The reduction

Scheme 1. Illustration of How Ag Nanoparticles Can Be Uniformly Dispersed along Nanosilicate Platelet with PU on Stainless Surface[a]

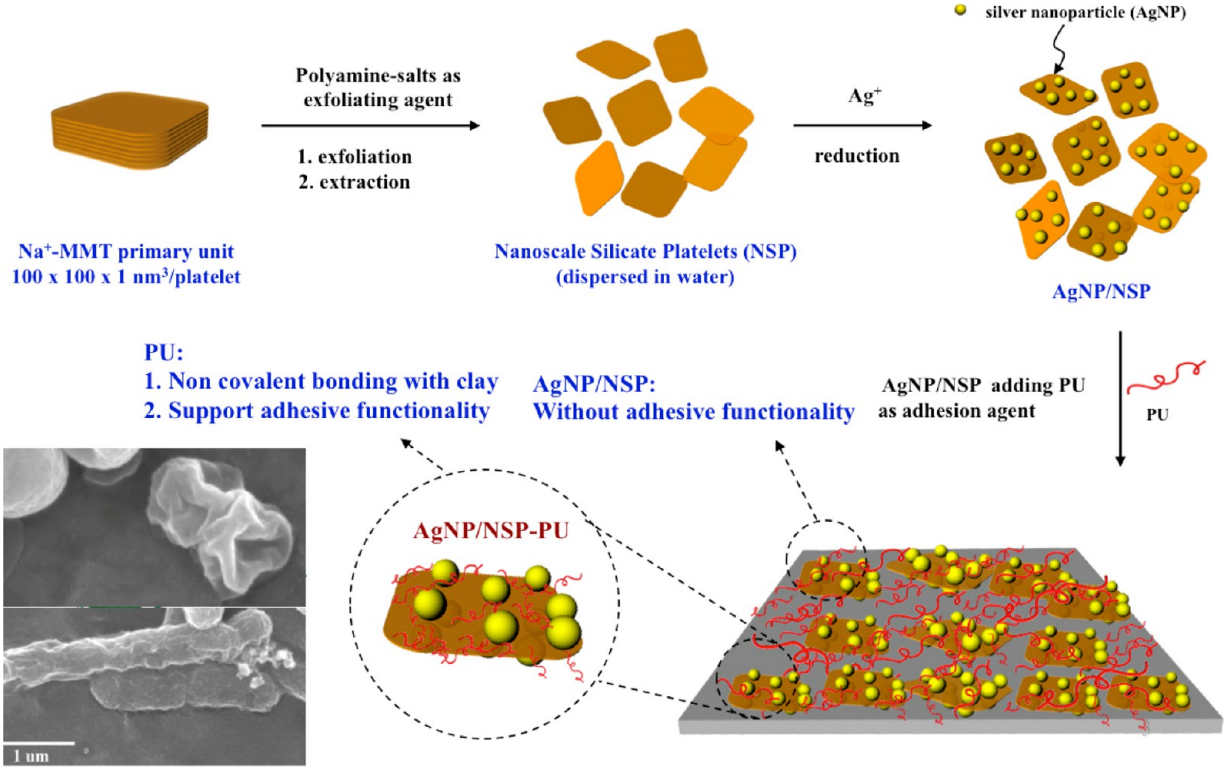

[a]Conceptual description of surface coating with AgNP/NSP−PU. Our results were exhibited on a trifunctional thin-film. These results show that the new tricomponent nanohybrid (AgNP/NSP−PU) with the ratio 1/3 of AgNP/NSP to PU had good bactericidal activity, lacked cytotoxicity, and had good adhesion property.

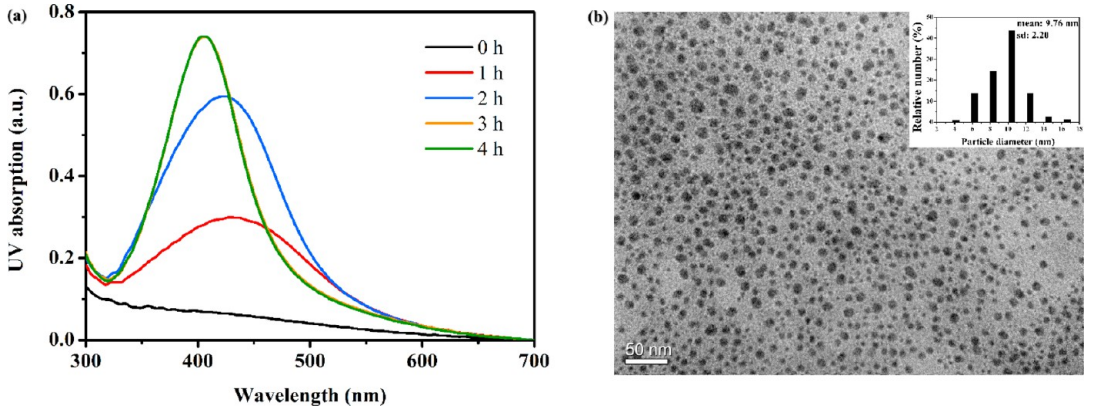

Figure 1. AgNP/NSP preparation and nanoparticle distribution; characterization by UV absorption and TEM for AgNP formation and size distribution. (a) UV−vis absorption at ~408 nm of the AgNP/NSP water solution, indicating the formation of Ag^0 in nanoparticle form; the kinetic increase of peak height indicates the AgNP concentration of the AgNP/NSP (7/93 w/w composition) samples; (b) TEM image of AgNP/NSP (7/93) and (inset) bar graph showing the average particle size to be ~9.76 ± 2.2 nm.

of 30% in comparison to the negative control was assumed to be the total inhibition of the mitochondrial activity.

3. RESULTS AND DISCUSSION

Although the silver ion (Ag^+)-based components are conventionally used for wound dressing, the toxicity of Ag^+ is generally concerning. The cytotoxicity risk is even more important for any medical devices and implants used in the human body. In this study, the design of the AgNP/NSP nanohybrid dispersed in water-based PU coating on the surface of stainless steel metal as the infection-free implants was thoroughly investigated for adhesive capacity, antimicrobial efficacy, and cell cytotoxicity (Scheme 1).

3.1. Characterization of AgNP/NSP Nanohybrid and AgNP/NSP−PU Tricomponent. The previously developed synthesis of AgNP/NSP nanohybrid is conceptually depicted in Scheme 1. NSP was prepared by the exfoliation of the layered structure of the clay and followed by the in situ reduction of silver nitrate into AgNP. The NSP were in the dimension of ca. 100 × 100 × 1 nm as the thin-platelet geometric shape, derived from the randomization of the natural clays such as sodium montmor-

dx.doi.org/10.1021/am5057213 | ACS Appl. Mater. Interfaces 2014, 6, 20324−20333

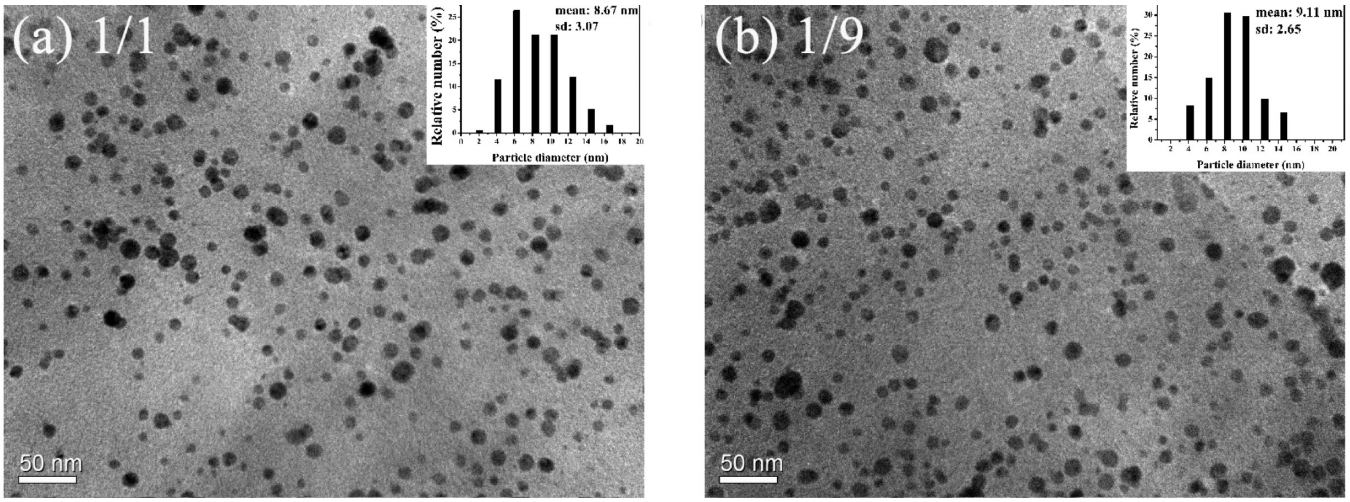

Figure 2. TEM characterization of AgNP/NSP in waterborne PU with even dispersion. (a) AgNP/NSP to PU ratio (1/1 by weight ratio of the nanohybrid to organic PU); (b) AgNP/NSP to PU ratio (1/9 by weight ratio); (insets) Ag size distributions by calculation of representative particle sizes with averages of (a) 8.67 ± 3.07 and (b) 9.11 ± 2.65 nm.

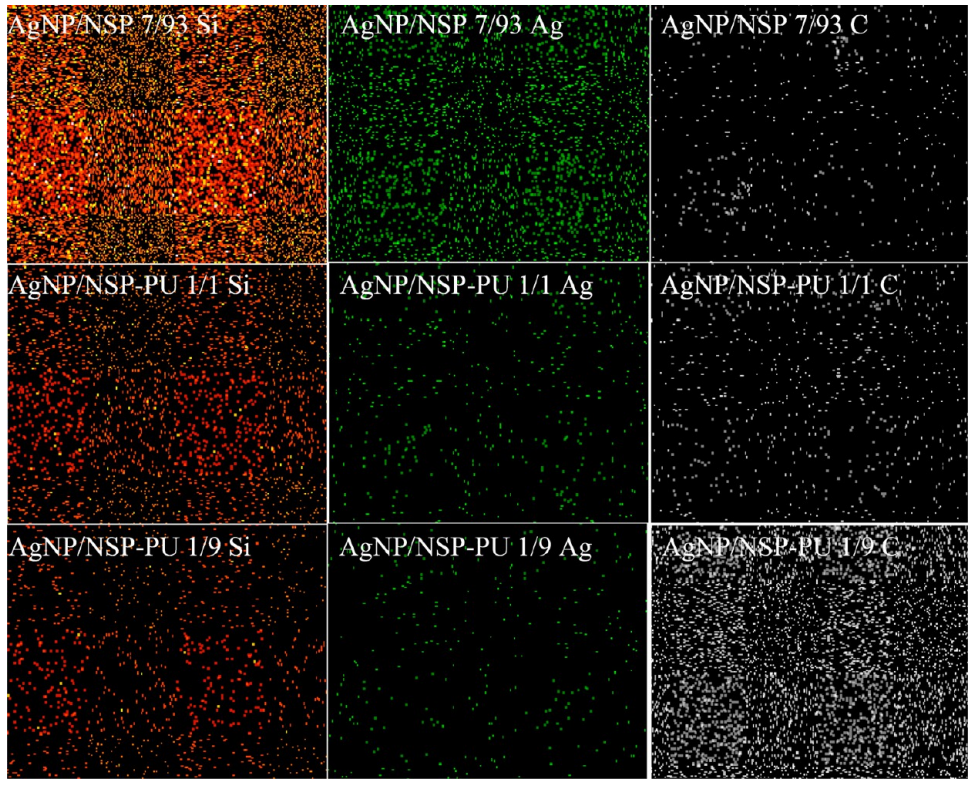

Figure 3. EDS images of AgNP/NSP−PU and AgNP/NSP showing that the particles of the nanohybrids are evenly distributed on the metal plate surface.

illonite. In the silver nitrate reduction, increasing the Ag weight fraction in the Ag/silicate composition from 7/93 to 50/50 (w/w) largely altered the particle size of AgNP from 3.6 to 35 nm in diameter.[31] In this study, 7/93 AgNP/NSP nanohybrid at the AgNP diameter of 9.76 nm was examined with TEM (Figure 1b). This product had the optimum absorption peak at 408 nm, and its kinetic change during the synthesis with increasing reaction time was recorded in Figure 1a. The AgNP/NSP nanohybrid was previously developed and synthesized. The particle size distributed was from 3.6 to 35 nm.[31] The weight ratio of AgNP to NSP at 7/93 (w/w) was selected due to its stability of preventing the release of Ag^+ from Ag^0 oxidation. The optimized AgNP/NSP nanohybrid of 7/93 (w/w) was utilized throughout this work. This Ag nanohybrid was characterized to have the maximum UV absorption of 408−409 nm. The characteristic peak absorption was used to monitor the reduction of $AgNO_3$ during the synthesis. The AgNP formation and nanoparticle size distribution were further evidenced by the direct observation by TEM micrographs, as shown in Figure 1. The average particle diameter was in the range of 4−17 nm and averaged 9.76 nm, as shown by TEM images. In literature, the generally larger size (50−300 nm) of nanoparticles was reported.[27,33] The differences

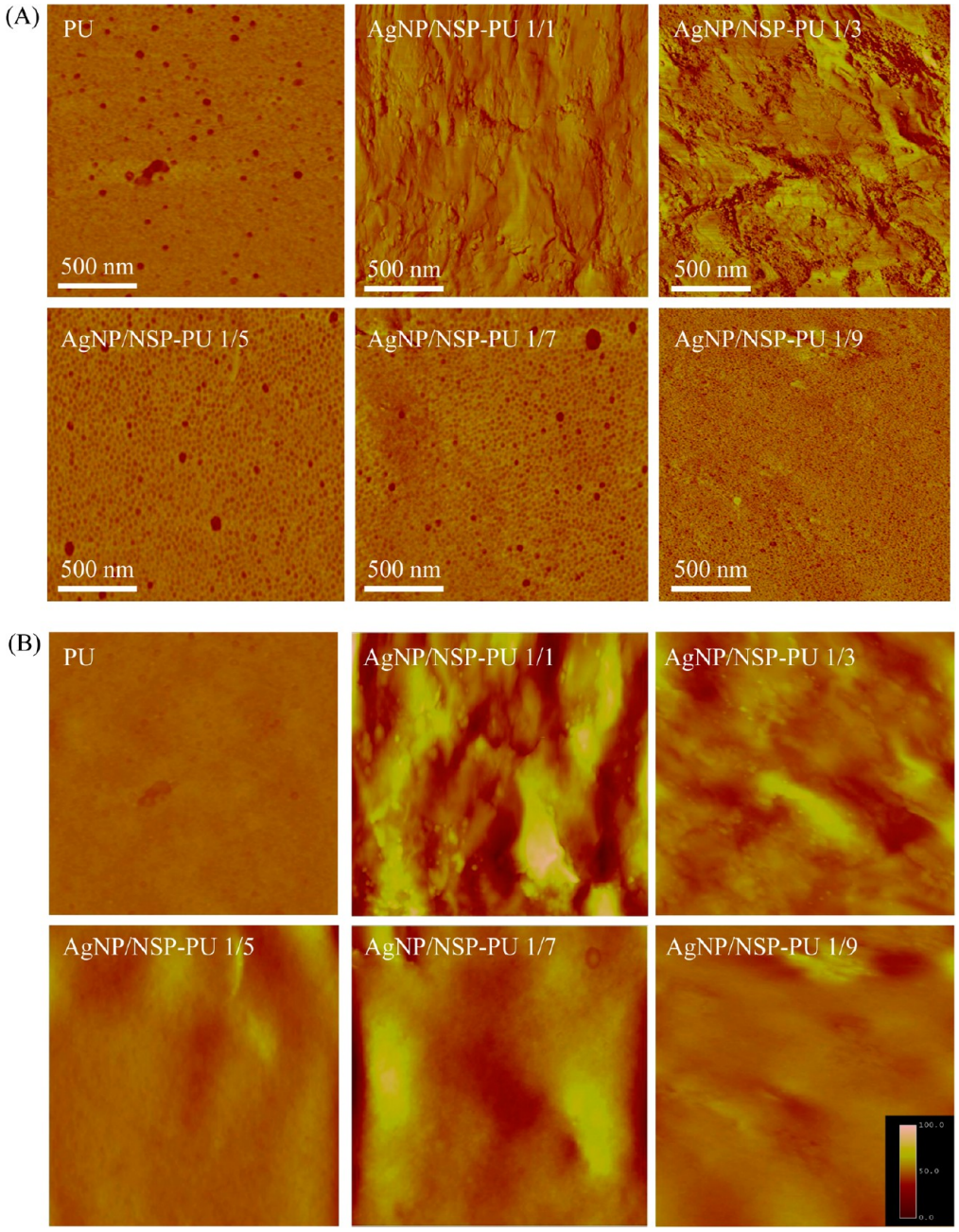

Figure 4. AFM tapping mode images of AgNP/NSP to PU weight ratios (the pristine PU and different weight ratios of 1/1 to 1/9 AgNP/NSP blended with PU and coated on metal plates (scan size 1 × 1 cm), showing their surface roughness); (A) phase images and (B) amplitude images. (B) Height scale bar is 100 nm for 1 cm^2 images.

in particle size could affect the bactericidal ability and toxicity of cell damage.[25,34]

For coating the Ag nanohybrid, we investigated the inhibition of bacterial growth on the medical device surface. To facilitate the surface coating smoothness, homogeneousness, and the Ag nanohybrid adhesion, we employed the waterborne polyurethane (PU) by blending technique. The selection of the suitable PU through the preliminary screening of the chemical component is described in the experimental procedures.

The waterborne PU was blended into AgNP/NSP (7/93 w/w) and used for coating on stainless steel plates. Various thicknesses of the coated films down to ∼1.5 μm were generated by casting the Ag slurry in PU suspension onto a 3 × 3 or 1 × 1 cm sample plate by drop casting method. The mean size of Ag particle size in the AgNP/NSP−PU dispersion was found to be 8.67−9.11 nm by TEM examination, as shown in Figure 2. We believe that our nanocomposites constitute the waterborne PU that governs a strong capacity for the coupling mechanism among the interaction of evenly distributed nanoparticles, nanosilicate platelets, and metal plates. The Ag particles size of the AgNP/NSP maintained the smaller size in the dispersions before (9.76 nm) and after (8.67−9.11 nm) the PU blending. For further promotion of the adhesion of AgNP/NSP on the metal plate, the involvement of waterborne PU was developed and became the tricomponent nanohybrid. The amount of PU in blending with AgNP/NSP (7/93) can be adjusted in a large range of weight ratios from 10/1 to 1/10 w/w. It was found that, in these different weight fractions of AgNP/NSP in PU, the

average Ag diameter remained in the range of 8.67−9.11 nm, regardless of the amount of PU addition. It was noticed that the Ag particle size was not affected by the PU addition, indicating the stability of AgNP/NSP (7/93) nanohybrid.

3.2. Characterization of AgNP/NSP−PU Tricomponent Coating Surface. The presence of the PU in the tricomponent nanohybrid could significantly enhance the adhesion of the Ag nanohybrid on the stainless steel surface. For the coating process, the AgNP/NSP in PU dispersion could be diluted to a suitable concentration and viscosity for coating onto metal plates.

Using EDS, the surface images represented the content of atoms and their locations on the metal. In this study, we used EDS to confirm that the AgNP/NSP−PU on the metal plates was truly homogeneous. The uniformity of the silver nanosilicate platelets of nanohybrid with waterborne PU were represented on the metal plates surface. Figure 3 shows AgNP/NSP with a ratio of 7/93 and AgNP/NSP−PU with ratios of 1/1 and 1/9 (w/w). Red spots indicate silicate atoms (NSP), green spots indicate silver atoms (AgNP), and white spots indicate carbon atoms (PU). Also, we found that AgNP/NSP had more silicate atoms than AgNP/NSP−PU (1/1, 1/9 w/w). At the ratio 1/9 (w/w), the carbon indicates the content of waterborne PU (white spots) spread on the metal plates homogeneously. Due to the dilution effect, the nanoparticle interspace increases, and there is no PU blending. We suppose that the Ag nanoparticle interspace may not be affected by our waterborne PU. It may evenly scatter nanoparticles over the coating surface.

NSP is used in the carrier of the nanoscale reduced-form AgNP on the surface area. In contrast, the reduced AgNPs were evenly distributed in the tricomponent (Figure 2), and Ag elements were evenly scattered on the PU carbon film with little aggregation (Figure 3). The mean AgNP particle sizes were also much smaller, mostly less than 10 nm. Our tricomponent Ag/silicate/PU results improved over the AgNP aggregation on NSP in previous results.[31] No sedimentation of the waterborne PU was observed for one month; the hydrophilic hydroxyl groups of waterborne PU extended AgNP/NSP onto the stainless surface. EDS indicated the sorption of PU on the nanosilicate existence of zerovalent silver (Ag^0) in the AgNP/NSP−PU mass, suggesting the formation of stable AgNP and even dispersion.

The AgNP/NSP−PU coating of the stainless steel surface was examined for the AFM topographical images. Figure 4 shows the smoothness of the PU surface without mixing with the Ag nanohybrid. Depending on the weight fraction of AgNP/NSP in PU, after the coating, the surface morphology could appear to be in high roughness, particularly when using a lower PU fraction (such as 1/1 and 1/3). The smooth surface similar to the pure PU coating was observed for the higher PU ratios (1/5, 1/7, and 1/9) in blending with the Ag nanohybrid. The roughness of the coated surface could be further correlated to the effectiveness of antimicrobial and material adhesion to the metal surface.[35] The intrinsic properties of NSPs, which include high surface-area-to-weight ratio, unique physical properties and morphology, and a high negative electrical conductivity, and their inherent size and flat geometry can make them extremely adept in expelling bacteria. When almost all bacteria cells grown in minimal media had a negative zeta potential, the AgNP/NSP−PU surface may possess the ability to prevent the bacteria attachment.[35]

3.3. Physical Property of AgNP/NSP−PU on Stainless Steel Coating. The use of the waterborne PU could lead to the homogeneity of the AgNP/NSP particle dispersion in the matrix of the polymer film and the adherence of Ag materials on metal plates (Figure 2). The transparent film of the pristine-PU-coated metal plates turned black and roughed the surface after being mixed with AgNP/NSP (7/93), in comparison to the pure-PU coating. Comparing coatings on 316L stainless steel handle-shaped implants (1 × 1 cm), the AgNP/NSP to PU (1/1) coating on stainless steel was black in color and had a smooth surface, and the PU-only coating was transparent and had a smooth surface.

The adhesion ability of the nanohybrid-coated PU surface on metal plates is demonstrated in Figure 5. The silver nanohybrid

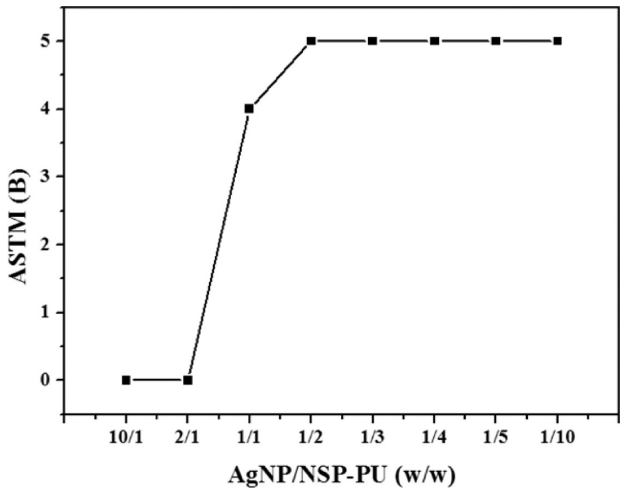

Figure 5. Cross-cut test of AgNP/NSP−PU coated on the stainless steel surface. Adherence ability of the AgNP/NSP−PU thin-film on a metal plate was represented according to ASTM D 3359: in *y* axis, 5B representing 0%, and 4B less than 5% of area possibly tearing off.

of homogeneous slurry in deionized water could be coated on the stainless steel implants in different thicknesses. The uses of AgNP/NSP−PU dispersion containing the compositions with higher fractions of waterborne PU in ratio could lead to a darker yellowish color and a higher strength in adhesion on the metal surface. We demonstrated the effectiveness of using the waterborne PU in mixing with nanoscale silicate platelets and AgNP/NSP smudges by the simple coating technique.

The uses of waterborne PU as the polymer medium to disperse the AgNP/NSP nanohybrid at various weight ratios (1/0.1, 1/0.5, 1/1, 1/2, 1/3, 1/4, 1/5, and 1/10) were prepared. The dilution can be further carried out by using deionized water to adjust the concentration and hence the coated film thickness. At the thickness as low as ∼1.5 μm on stainless steel plates (1 × 1 cm), the high adhesion strength was obtained for the composition ratio of 1/2, 1/3, 1/4, 1/5, and 1/10 in PU-rich solutions, while relatively low strength was shown for the composition with less PU, such as the weight ratios of 2/1 to 10/1. The adherent ability is shown in Figure 5. The relative strength against the surface scratching was presented on the basis of the cross-cut test according to ASTM D 3359. The adhesion was proportionally related to the fraction of PU in the tricomponent coating. According to our data and Table 1, the weight ratio of AgNP/NSP to PU at 1/2 had a strength that fell under the 5B category in the cross-cut test. It appeared that the composition of using PU over 1/2 ratio was the critical point for achieving the maximum 5B adhesiveness. The presence of a suitable amount of waterborne PU became necessary for achieving the adhesiveness of Ag on the stainless steel.

3.4. Antibacterial Efficacy of AgNP/NSP−PU Coating Surface and SEM Analyses. According our tricomponent design, the negative conductivity of NSP against the bacterial attachment, the AgNP bactericidal activity, the waterborne PU adhesive ability, and the coating surface of AgNP/NSP−PU will exhibit the higher antibacterial efficiency. The antimicrobial efficacy of the metal surface is summarized in Figure 6, showing

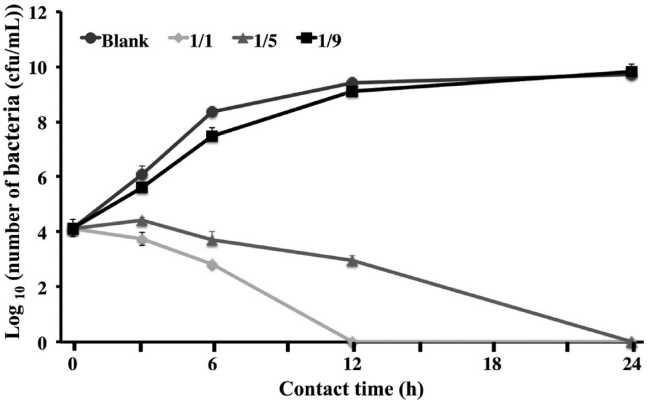

Figure 6. Bactericidal activity of AgNP/NSP−PU films surface. Results of AgNP/NSP to PU coating surface at weight ratios of 1/1, 1/5, and 1/9 and blank metal plates after exposure to *S. aureus* at 37 °C for 3−24 h to show the effectiveness of bacterial inhibition for 1/1 and 1/5 while maintaining the same growth curve for the composition of the 1/9 ratio with blank.

the inhibition of bacterial growth for the composition coating of 1/1 and 1/5 ratios of AgNP/NSP to PU. The tests were performed by putting the coated metal plates in contact with *S. aureus* for an incubation period of 24 h. By comparison, the coated film with the composition of 1/9 weight ratio had shown no antimicrobial activity. In the control experiments and 1/9 ratio, the bacteria were visible during the 24 h growth period. These observations indicated the relative degree of bactericidal activity of AgNP. By comparison with the control (blank with no Ag coating), some bacterial growth occurred on the surface of the high-PU (i.e., 1/9) coating. For the 1/1 and 1/5 coatings, almost no bacterial growth occurred, as shown in Figure 6. The homogeneous dispersion of AgNP/NSP in the waterborne PU at the proper weight ratio was blended and coated on metal plates. The antibacterial efficacy is mainly unaffected by even Ag dispersion but was affected by the composition of Ag in PU films. The bacterial survival was dramatically reduced by contact with the 1/1 AgNP/NSP to PU film.

For further functional characterization of coating surface by tricomponent of AgNP/NSP−PU, the antimicrobial efficacy of the metal surface was optimum Ag nanoparticle in Figure 6, showing the bacterial inhibition. In the previous studies, the bactericidal function of AgNP/NSP was revealed for inhibiting bacterial strains including *S. aureus*, *Escherichia coli*, and *Salmonella enteric*.[30,31,36] In this study, the PU was blended in the tricomponent AgNP/NSP−PU which was subsequently coated on the metal plate. The plate surface was then examined for its antimicrobial behavior against the growth of *S. aureus*. In our experiment, the coating with no PU and the low-Ag nanohybrid were shown to be negative for inhibition or the continuing growth of bacteria on the smooth surface of PU and 1/9, as shown in Figure 4. It was also found that the micrograph of surface roughness of our coating on the metal plate was varied by the PU fraction and, consequently, by the antimicrobial behavior in contacting microorganisms.[35]

To further demonstrate the antibacterial activity of 1/1 and 1/5 ratios of AgNP/NSP−PU surface (Figure 6), we also verified the antibacterial activity on the same surface by LIVE/DEAD analysis of the 1/1 and 1/5 groups (Figure 7). The antibacterial

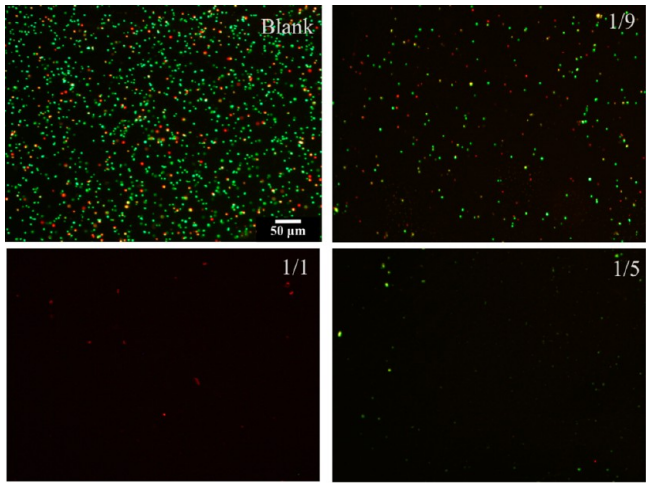

Figure 7. Bactericidal LIVE/DEAD analysis. Growth of *S. aureus* (after exposure for 12 h) on AgNP/NSP−PU coating on stainless steel surface; bacteria disappear in 1/1 and 1/5 compositions, and more green spots appear on the 1/9 PU-rich surface.

activities could be further evidenced by visualizing the LIVE/DEAD stain method, where green indicates viable cells and red for nonviable cells. The bacterial growth was totally inhibited for the coated surface with AgNP/NSP-to-PU ratios of 1/1−1/5. Among these tests, the compositions of 1/1−1/5 AgNP/NSP to PU weight ratios demonstrated the antibacterial activity. The antibacterial efficacy was proportionally lowered by increasing the PU component. In optimizing the PU adherent ability and the promoting AgNP/NSP bactericidal activity, the weight ratio of 1/1 to 1/3 for the AgNP/NSP-to-PU blend was found.

Both bacterial growth inhibition and bacterial survival were identifiable in SEM micrographs. Furthermore, the direct contact of the film surface with bacterial population could be visualized by using field emission-scanning electron microscopy (FE-SEM). The incubation of *S. aureus* on the Ag nanohybrid coated films was confirmed, and the SEM images of the bacterial contact after 24 h are shown in Figure 8. The loosely scattered bacteria debris appeared on the surface of the Ag-treated 1/1 surface, whereas the 1/9 surface had large amount of live bacterial aggregates consistent with the bacterial count results shown in Figures 6 and 7.

3.5. Cytotoxicity of the AgNP/NSP−PU Nanocomposites. For the safety test, AgNP/NSP to PU (1/1) at a concentration of up to 10 ppm was shown to be nontoxic to the mouse fibroblasts with ISO 10993-5 protocol. The tested concentration of the silver nanohybrid was effective for exhibiting nearly complete bacterial growth reduction. Hence, the biocompatibility and the minimum cytotoxicity were clearly demonstrated for this specific nanohybrid in the waterborne PU, shown in as Figure 9.

The conventional AgNP was studied for its safety issues in addition to its antimicrobial activities.[25,27,33,37] The AgNP/NSP blended with food diets were demonstrated for the biocompatibility and antimicrobial activities in vivo and in vitro.[31,38,39]

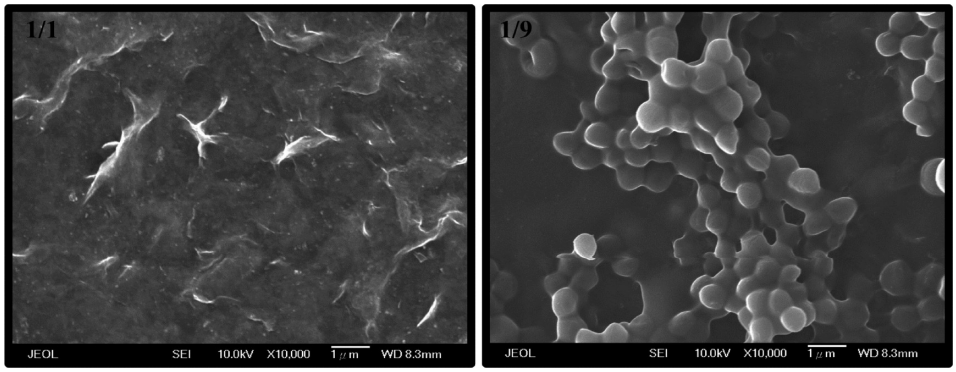

Figure 8. Bactericidal activity. SEM images are correlated to the samples under incubation for 24 h period for observing (right) the bacterial growth on 1/9 and (left) the bacterial disappearance on 1/1 composition surface.

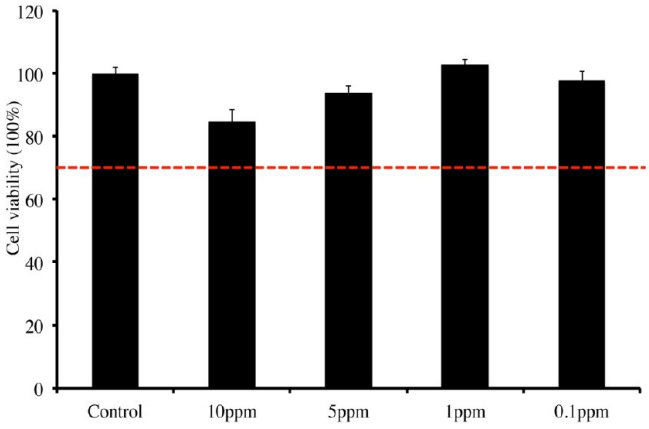

Figure 9. Mammalian cytotoxicity of the AgNP/NSP−PU tricomponent. Mammalian cell toxicity (or viability for 3T3 cells) of AgNP/NSP to PU (1/1 w/w) performed by the method according to ISO 10993-5; the safety level is indicated by the dashed red line.

Here, we address the safety issue of the PU-blended AgNP/NSP nanohybrid at a 1/1 ratio. The cytotoxicity with mammalian cells was tested by a AgNP/NSP−PU coating amount of 10 mg on the surface area (1 cm^2) of the stainless steel plate in our research. We assume that all surface coatings are subject to lyse and release all under the biodegradation in the body. The cytotoxicity of total release of AgNP/NSP−PU (10 ppm, 10 mg/kg) was tested in mammalian cells. Even at a 10-fold scale, the result of 100 ppm appeared to have no cytotoxicity or effect on the cell count (OD570) in our results. The cytotoxicity test of 100 ppm of AgNP/NSP−PU nanocomposites has shown to still be safe (70% cell viability) for the 24 h treatment period. The data indicated the mildness of the Ag nanohybrid in waterborne PU with respect to the growth of mammalian cells. Overall, the developed AgNP/NSP-to-PU ratios of 1/1−1/3 nanohybrid had even distribution over the surface of nanoparticles and high adhesive ability on the metal plate, as shown in Figure 5; a unique property of antimicrobial activities, as shown in Figure 6; and omittable toxicity to mammalian cells, as shown in Figure 9.

4. CONCLUSIONS

In conclusion, the novel tricomponent AgNP/NSP−PU was successfully developed by homogeneously blending Ag/silicate nanohybrid in the selected type of waterborne PU. The weight ratio of AgNP/NSP to PU was optimized at the composition of 1/1 to 1/5 for both of antimicrobial efficacy and coating adhesiveness. The presence of PU is necessary for enhancing the coating adhesion and even dispersion of immobilizing Ag on the metal surface and enhancing antimicrobial efficacy due to the Ag distribution of AgNP. In considering the biocompatibility, the tricomponent AgNP/NSP-to-PU (1/1 w/w) was found to omit cytotoxicity mammalian cells. Hence, the metal surface with the functions of high antimicrobial efficacy and less cytotoxicity could be achieved. The optimized compositions of AgNP/NSP to PU (1/1 to 1/3 w/w) were suitable for the coating. It was further demonstrated that a film thickness as low as 1.5 μm was enough for exhibiting the durable composite surface with a good microbiocide property. The findings will impact the field of designing medical devices with antimicrobial function and medical safety.

AUTHOR INFORMATION

Corresponding Author

*E-mail: mike920@gmail.com. Tel: 886-2-23123456, 65987. Fax: 886-2-23224112.

Author Contributions

[⊥]Yi-Hsiu Huang and Mark Hung-Chih Chen contributed equally. The manuscript was written through contributions of all authors. All authors have given approval to the final version of the manuscript.

Notes

The authors declare no competing financial interest.

ACKNOWLEDGMENTS

We gratefully acknowledge the financial supports from the Ministry of Science and Technology of Taiwan (101-2622-B-002-007-CC3), the Ministry of Economic Affairs of Taiwan, National Taiwan University Hospital (NTUH.102-S2144) and E-Da Hospital—National Taiwan University Hospital Joint Research Program (102-EDN13).

ABBREVIATIONS

EDS, energy dispersive spectroscopy
AFM, atomic force microscope
TEM, transmission electron microscope
FE-SEM, field emission-scanning electron microscopy
ASTM, American Society for Testing and Materials
NSP, nano-silicate platelet
AgNP, silver nanoparticles
PU, polyurethane

REFERENCES

(1) Williams, D. L.; Haymond, B. S.; Woodbury, K. L.; Beck, J. P.; Moore, D. E.; Epperson, R. T.; Bloebaum, R. D. Experimental Model of Biofilm Implant-Related Osteomyelitis to Test Combination Biomaterials Using Biofilms as Initial Inocula. *J. Biomed. Mater. Res., Part A* **2012**, *100*, 1888−1900.

(2) Zhao, Q.; Liu, Y.; Wang, C.; Wang, S.; Peng, N.; Jeynes, C. Bacterial Adhesion on Ion-Implanted Stainless Steel Surfaces. *Appl. Surf. Sci.* **2007**, *253*, 8674−8681.

(3) Wan, Y. Z.; Raman, S.; He, F.; Huang, Y. Surface Modification of Medical Metals by Ion Implantation of Silver and Copper. *Vacuum* **2007**, *81*, 1114−1118.

(4) Ishihara, M.; Kosaka, T.; Nakamura, T.; Tsugawa, K.; Hasegawa, M.; Kokai, F.; Koga, Y. Antibacterial Activity of Fluorine Incorporated DLC Films. *Diamond Relat. Mater.* **2006**, *15*, 1011−1014.

(5) Arita, N. K.; Shinonaga, Y.; Nishino, M. Plasma-Based Fluorine Ion Implantation into Dental Materials for Inhibition of Bacterial Adhesion. *Dent. Mater. J.* **2006**, *25*, 684−692.

(6) Yoshinari, M.; Oda, Y.; Kato, T.; Okuda, K. Influence of Surface Modifications to Titanium on Antibacterial Activity in Vitro. *Biomaterials* **2001**, *22*, 2043−2048.

(7) Su, C. T.; Yuan, R. H.; Chen, Y. C.; Lin, T. J.; Chien, H. W.; Hsieh, C. C.; Tsai, W. B.; Chang, C. H.; Chen, H. Y. A Facile Approach toward Protein-Resistant Biointerfaces Based on Photodefinable Poly-*p*-xylylene Coating. *Colloids Surf., B* **2014**, *116*, 727−733.

(8) Su, H. L.; Chou, C. C.; Hung, D. J.; Lin, S. H.; Pao, I. C.; Lin, J. H.; Huang, F. L.; Dong, R. X.; Lin, J. J. The Disruption of Bacterial Membrane Integrity through ROS Generation Induced by Nanohybrids of Silver and Clay. *Biomaterials* **2009**, *30*, 5979−5987.

(9) Min, Y.; Akbulut, M.; Kristiansen, K.; Golan, Y.; Israelachvili, J. The Role of Interparticle and External Forces in Nanoparticle Assembly. *Nat. Mater.* **2008**, *7*, 527−538.

(10) Rifai, S.; Breen, C. A.; Solis, D. J.; Swager, T. M. Facile in Situ Silver Nanoparticle Formation in Insulating Porous Polymer Matrices. *Chem. Mater.* **2006**, *18*, 21−25.

(11) Wildgoose, G. G.; Banks, C. E.; Compton, R. G. Metal Nanoparticles and Related Materials Supported on Carbon Nanotubes: Methods and Applications. *Small* **2006**, *2*, 182−193.

(12) Korchev, A. S.; Bozack, M. J.; Slaten, B. L.; Mills, G. Polymer-Initiated Photogeneration of Silver Nanoparticles in SPEEK/PVA Films: Direct Metal Photopatterning. *J. Am. Chem. Soc.* **2004**, *126*, 10−11.

(13) Zheng, M. P.; Gu, M. Y.; Jin, Y. P.; Jin, G. L. Optical Properties of Silver-Dispersed PVP Thin Film. *Mater. Res. Bull.* **2001**, *36*, 853−859.

(14) Chen, M. H.; Hsu, L. C.; Wu, J. L.; Yeh, C. W.; Tsai, J. N.; Hseu, Y. C.; Hsu, L. S. Exposure to Benzidine Caused Apoptosis and Malformation of Telencephalon Region in Zebrafish. *Environ. Toxicol.* **2013**, *28*, 1−9.

(15) Heuser, V. D.; de Andrade, V. M.; da Silva, J.; Erdtmann, B. Comparison of Genetic Damage in Brazilian Footwear-Workers Exposed to Solvent-Based or Water-Based Adhesive. *Mutat. Res., Genet. Toxicol. Environ. Mutagen.* **2005**, *583*, 85−94.

(16) Chang, Y. C.; Chou, C. C.; Lin, J. J. Emulsion Intercalation of Smectite Clays with Comb-Branched Copolymers Consisting of Multiple Quaternary Amine Salts and a Poly(styrene-butadiene-styrene) Backbone. *Langmuir* **2005**, *21*, 7023−7028.

(17) Lin, J.-J.; Dong, R.-X.; Tsai, W.-C. High Surface Clay-Supported Silver Nanohybrids Silver Nanoparticles. In *Silver Nanoparticles*; Perez, D. P., Ed.; InTech: Rijeka, Croatia, 2010; pp 161−176.

(18) Falentin-Daudre, C.; Faure, E.; Svaldo-Lanero, T.; Farina, F.; Jerome, C.; Van De Weerdt, C.; Martial, J.; Duwez, A. S.; Detrembleur, C. Antibacterial Polyelectrolyte Micelles for Coating Stainless Steel. *Langmuir* **2012**, *28*, 7233−7241.

(19) Dong, Y.; Li, X.; Tian, L.; Bell, T.; Sammons, R. L.; Dong, H. Towards Long-Lasting Antibacterial Stainless Steel Surfaces by Combining Double Glow Plasma Silvering with Active Screen Plasma Nitriding. *Acta Biomater.* **2011**, *7*, 447−457.

(20) Miola, M.; Ferraris, S.; Di Nunzio, S.; Robotti, P. F.; Bianchi, G.; Fucale, G.; Maina, G.; Cannas, M.; Gatti, S.; Masse, A.; Vitale Brovarone, C.; Verne, E. Surface Silver-Doping of Biocompatible Glasses to Induce Antibacterial Properties. Part Ii: Plasma Sprayed Glass-Coatings. *J. Mater. Sci.: Mater. Med.* **2009**, *20*, 741−749.

(21) Devasconcellos, P.; Bose, S.; Beyenal, H.; Bandyopadhyay, A.; Zirkle, L. G. Antimicrobial Particulate Silver Coatings on Stainless Steel Implants for Fracture Management. *Mater. Sci. Eng., C* **2012**, *32*, 1112−1120.

(22) Su, H. L.; Lin, S. H.; Wei, J. C.; Pao, I. C.; Chiao, S. H.; Huang, C. C.; Lin, S. Z.; Lin, J. J. Novel Nanohybrids of Silver Particles on Clay Platelets for Inhibiting Silver-Resistant Bacteria. *PLoS One* **2011**, *6*, e21125.

(23) Shinonaga, Y.; Arita, K. Antibacterial Effect of Acrylic Dental Devices after Surface Modification by Fluorine and Silver Dual-Ion Implantation. *Acta Biomater.* **2012**, *8*, 1388−1393.

(24) Ren, N.; Li, R.; Chen, L.; Wang, G.; Liu, D.; Wang, Y.; Zheng, L.; Tang, W.; Yu, X.; Jiang, H.; Liu, H.; Wu, N. In Situ Construction of a Titanate−Silver Nanoparticle−Titanate Sandwich Nanostructure on a Metallic Titanium Surface for Bacteriostatic and Biocompatible Implants. *J. Mater. Chem.* **2012**, *22*, 19151−19160.

(25) Park, M. V.; Neigh, A. M.; Vermeulen, J. P.; de la Fonteyne, L. J.; Verharen, H. W.; Briede, J. J.; van Loveren, H.; de Jong, W. H. The Effect of Particle Size on the Cytotoxicity, Inflammation, Developmental Toxicity, and Genotoxicity of Silver Nanoparticles. *Biomaterials* **2011**, *32*, 9810−9817.

(26) AshaRani, P. V.; Low Kah Mun, G.; Hande, M. P.; Valiyaveettil, S. Cytotoxicity and Genotoxicity of Silver Nanoparticles in Human Cells. *ACS Nano* **2009**, *3*, 279−290.

(27) Roy, N.; Gaur, A.; Jain, A.; Bhattacharya, S.; Rani, V. Green Synthesis of Silver Nanoparticles: An Approach to Overcome Toxicity. *Environ. Toxicol. Pharmacol.* **2013**, *36*, 807−812.

(28) Hadrup, N.; Lam, H. R. Oral Toxicity of Silver Ions, Silver Nanoparticles, and Colloidal Silver—A Review. *Regul. Toxicol. Pharmacol.* **2014**, *68*, 1−7.

(29) Ge, L.; Li, Q.; Wang, M.; Ouyang, J.; Li, X.; Xing, M. M. Nanosilver Particles in Medical Applications: Synthesis, Performance, and Toxicity. *Int. J. Nanomed.* **2014**, *9*, 2399−2407.

(30) Wei, J. C.; Yen, Y. T.; Wang, Y. T.; Hsu, S. H.; Lin, J. J. Enhancing Silver Nanoparticle and Antimicrobial Efficacy by the Exfoliated Clay Nanoplatelets. *RSC Adv.* **2013**, *3*, 7392−7397.

(31) Lin, J. J.; Lin, W. C.; Li, S. D.; Lin, C. Y.; Hsu, S. H. Evaluation of the Antibacterial Activity and Biocompatibility for Silver Nanoparticles Immobilized on Nano Silicate Platelets. *ACS Appl. Mater. Interfaces* **2013**, *5*, 433−443.

(32) Lin, J. J.; Chu, C. C.; Chiang, M. L.; Tsai, W. C. First Isolation of Individual Silicate Platelets from Clay Exfoliation and Their Unique Self-Assembly into Fibrous Arrays. *J. Phys. Chem. B* **2006**, *110*, 18115−18120.

(33) Rai, M.; Yadav, A.; Gade, A. Silver Nanoparticles as a New Generation of Antimicrobials. *Biotechnol. Adv.* **2009**, *27*, 76−83.

(34) Morones, J. R.; Elechiguerra, J. L.; Camacho, A.; Holt, K.; Kouri, J. B.; Ramirez, J. T.; Yacaman, M. J. The Bactericidal Effect of Silver Nanoparticles. *Nanotechnology* **2005**, *16*, 2346−2353.

(35) Campoccia, D.; Montanaro, L.; Arciola, C. R. A Review of the Biomaterials Technologies for Infection-Resistant Surfaces. *Biomaterials* **2013**, *34*, 8533−54.

(36) Chu, C. Y.; Peng, F. C.; Chiu, Y. F.; Lee, H. C.; Chen, C. W.; Wei, J. C.; Lin, J. J. Nanohybrids of Silver Particles Immobilized on Silicate Platelet for Infected Wound Healing. *PLoS One* **2012**, *7*, e38360.

(37) Asharani, P. V.; Hande, M. P.; Valiyaveettil, S. Anti-Proliferative Activity of Silver Nanoparticles. *BMC Cell Biol.* **2009**, *10*, 65.

(38) Chi, T. Y.; Yeh, H. Y.; Lin, J. J.; Jeng, U. S.; Hsu, S. H. Amphiphilic Silver-Delaminated Clay Nanohybrids and Their Composites with Polyurethane: Physico-Chemical and Biological Evaluations. *J. Mater. Chem. B* **2013**, *1*, 2178−2189.

(39) Chiao, S. H.; Lin, S. H.; Shen, C. I.; Liao, J. W.; Bau, I. J.; Wei, J. C.; Tseng, L. P.; Hsu, S. H.; Lai, P. S.; Lin, S. Z.; Lin, J. J.; Su, H. L. Efficacy and Safety of Nanohybrids Comprising Silver Nanoparticles and Silicate Clay for Controlling Salmonella Infection. *Int. J. Nanomed.* **2012**, *7*, 2421−2432.